

Efficient method for lasing eigenvalue problems of periodic structures

Yuxia Huang^a and Ya Yan Lu^{b,*}

^a*Department of Mathematics, Hangzhou Normal University, Hangzhou 310036, China*

^b*Department of Mathematics, City University of Hong Kong, Kowloon, Hong Kong*

(29 November 2013)

Lasing eigenvalue problems (LEPs) are non-conventional eigenvalue problems involving the frequency and gain threshold at the onset of lasing directly. Efficient numerical methods are needed to solve LEPs for the analysis, design and optimization of microcavity lasers. Existing computational methods for two-dimensional LEPs include the multipole method and the boundary integral equation method. In particular, the multipole method has been applied to LEPs of periodic structures, but it requires sophisticated mathematical techniques for evaluating slowly converging infinite sums that appear due to the periodicity. In this paper, a new method is developed for periodic LEPs based on the so-called Dirichlet-to-Neumann maps. The method is efficient since it avoids the slowly converging sums and can easily handle periodic structures with many arrays.

Keywords: Lasing eigenvalue problem, numerical method, Dirichlet-to-Neumann map.

1. Introduction

Lasers based on microcavities are highly attractive due to their small size, low power consumption, and potentially high modulation speed [1–3]. For analyzing a microcavity laser, it is often necessary to calculate the eigenmodes of the microcavity. These modes are solutions of the linear frequency-domain Maxwell's equations without sources and incident waves, and they usually exist at some complex frequencies. The real and imaginary parts of the complex frequency ω_* give the resonant frequency and the decay rate in time, respectively. The Q factor of the resonant mode can be calculated by $0.5|\operatorname{Re}(\omega_*)/\operatorname{Im}(\omega_*)|$. Eigenmodes with the largest Q factors are usually associated with lasing. However, the Q -factor theory based on the eigenmodes of the passive microcavity does not take into account how the active media is pumped and gives no value for the gain threshold of lasing. The lasing eigenvalue problem (LEP) formulation [4, 5] is a simple approach to overcome the above limitations. As in earlier works [6], an imaginary

*Corresponding author. Email: mayylu@cityu.edu.hk

part γ is added to the refractive index (or the dielectric constant) in the active region to model optical gain. The LEP is solved to determine the lasing frequency and the gain threshold for the onset of lasing. More precisely, we determine a real frequency ω (or wavenumber k_0) and a real γ , such that the homogeneous Maxwell's equations have a non-zero solution satisfying proper outgoing radiation conditions.

The eigenvalue problem of a passive cavity can be solved by many different numerical methods. Mathematically, these methods can be classified as linear and nonlinear ones. A linear method gives rise to a linear matrix eigenvalue problem (ω_* or ω_*^2 is the eigenvalue) through a discretization of the spatial variables or an expansion of the unknown eigenfunction in a series. A nonlinear method produces an equation $\mathbf{F}(\omega_*)\mathbf{u} = \mathbf{0}$, where \mathbf{F} is a matrix, \mathbf{u} is a vector related to the eigenfunction, and ω_* appears implicitly in \mathbf{F} . The multipole method [10, 12] and the boundary integral equation (BIE) method [13, 14] are well known nonlinear methods. For the multipole method, the electromagnetic field of the eigenmode is written as a sum of cylindrical or spherical waves which depend on ω_* , and \mathbf{u} is a vector for the unknown coefficients. For the BIE method, the integral operators are related to the Green's function which depends on ω_* , and \mathbf{u} represents some electromagnetic field components on material interfaces or some unknown density functions. To solve the nonlinear eigenvalue problem, we find ω_* from the condition that \mathbf{F} is a singular matrix, and determine \mathbf{u} as a non-zero solution of the system. The nonlinear methods are useful, since the size of matrix \mathbf{F} is often much smaller than the size of the matrices that appear in linear methods.

The LEPs are non-conventional eigenvalue problems, since an "eigenvalue" is not one (in general complex) number, but a pair of real numbers. Although the governing equations are still the linear frequency-domain Maxwell's equations, an LEP cannot be approximated by a linear matrix eigenvalue problem. However, we can still develop nonlinear methods for LEPs. A nonlinear method for an LEP gives rise to

$$\mathbf{F}(k_0, \gamma)\mathbf{u} = \mathbf{0}, \quad (1)$$

where the pair (k_0, γ) can be determined such that the matrix $\mathbf{F}(k_0, \gamma)$ is singular. Both multipole and BIE methods have been successfully applied to solve LEPs [7, 8]. Notice that k_0 and γ appear implicitly in the matrix \mathbf{F} , since the cylindrical or spherical waves and the Green's function depend on both of them.

LEPs for infinite periodic structures are also of interest, since periodic structures, such as diffraction gratings and photonic crystals (PhCs), have found many applications in light-emitting devices. Byelobrov *et al.* [9] studied an LEP for an infinite periodic array of circular cylinders

where the cylinders model quantum wires made of gain materials. They applied the multipole method to the LEP. For periodic structures involving circular cylinders, the multipole method uses cylindrical wave expansions and requires techniques for evaluating some slowly converging lattice sums [10]. While many methods have been developed for evaluating lattice sums [11], it is still desirable to avoid them. In an early work [15], we developed the so-called Dirichlet-to-Neumann (DtN) map method for computing transmission and reflection spectra of infinite periodic arrays of circular cylinders. Like the multipole method, the DtN-map method uses the fast converging cylindrical wave expansion, but it works in one period and does not require lattice sums. The DtN-map method has found many applications for analyzing PhC structures and devices [16–20]. In particular, it has been used to study passive PhC microcavities [21]. In this paper, we apply the DtN-map method to LEPs. Numerical examples indicate that the method is efficient and accurate for LEPs involving infinite periodic arrays of cylinders.

2. Lasing eigenvalue problem

We consider two-dimensional (2D) problems where the structure is described by a z -independent refractive index function $\eta = \eta(x, y)$, $\{x, y, z\}$ is a Cartesian coordinate system, the electromagnetic field and the pump are independent of z . To model gain in the active media and the spatial distribution of the pump, we introduce a material gain parameter γ , a function $\Gamma(x, y)$, and add $-i\gamma\Gamma(x, y)$ to the refractive index. This leads to the modified refractive index $n(x, y)$ and modified dielectric function $\varepsilon(x, y)$ satisfying

$$n(x, y) = \eta(x, y) - i\gamma\Gamma(x, y), \quad \varepsilon(x, y) = n^2(x, y). \quad (2)$$

The function Γ represents where the pump is applied. In the simplest case, we have $\Gamma = 1$ in the active region and $\Gamma = 0$ otherwise. Alternatively, we may add $-i\gamma\Gamma(x, y)$ to η^2 (the dielectric function) directly, then the modified dielectric function is

$$\varepsilon(x, y) = \eta^2(x, y) - i\gamma\Gamma(x, y). \quad (3)$$

Of course, the γ in (2) and the γ in (3) are different, but they can be approximately related to each other when their values are small. For simplicity, we only state the problem and present our method for the first model given in (2).

For the E and H polarizations, the governing equations are

$$\frac{\partial^2 u}{\partial x^2} + \frac{\partial^2 u}{\partial y^2} + k_0^2 \varepsilon u = 0, \quad (4)$$

$$\frac{\partial}{\partial x} \left(\frac{1}{\varepsilon} \frac{\partial u}{\partial x} \right) + \frac{\partial}{\partial y} \left(\frac{1}{\varepsilon} \frac{\partial u}{\partial y} \right) + k_0^2 u = 0, \quad (5)$$

where k_0 is the free space wavenumber, u is the z component of the electric or magnetic field. In the above, we have assumed a time dependence $e^{-i\omega t}$, thus absorption or gain are modeled by adding a positive or negative imaginary part to the refractive index, respectively. An LEP for 2D E or H polarization is to find real numbers k_0 and γ , and non-zero solutions u for Eq. (4) or (5) satisfying suitable outgoing radiation conditions. In that case, γ represents the gain threshold for the onset of lasing.

If the structure is surrounded by a homogeneous passive medium, i.e., $\eta = n_0$ and $\Gamma = 0$ when $r = \sqrt{x^2 + y^2}$ is sufficiently large, then the standard Sommerfeld radiation condition is applicable, i.e.,

$$\sqrt{r} \left(\frac{\partial u}{\partial r} - ik_0 n_0 u \right) \rightarrow 0, \quad r \rightarrow \infty. \quad (6)$$

We are interested in structures that are periodic in x and bounded by homogeneous passive media in y . For a simple example, we show a structure with three infinite periodic arrays of circular cylinders in Fig. 1. For such a periodic LEP, the outgoing radiation conditions are identical to

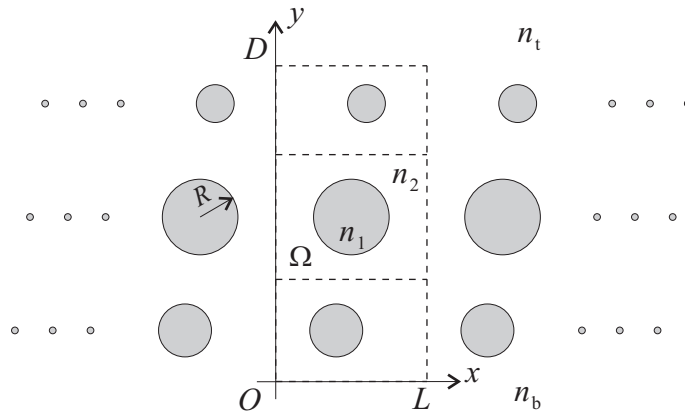


Figure 1. Three infinite periodic arrays of circular cylinders.

those for diffraction gratings [22]. More precisely, if $\eta(x, y)$, $\Gamma(x, y)$ and the solution $u(x, y)$ are all periodic in x with period L , and if the periodic structure is bounded in y as $0 < y < D$ such that $\eta = n_t$ and $\Gamma = 0$ for $y > D$, and $\eta = n_b$ and $\Gamma = 0$ for $y < 0$, where n_t and n_b are

constants, then u can be expanded as

$$u(x, y) = \sum_{m=-\infty}^{+\infty} C_{t,m} e^{i[\alpha_m x + \beta_{t,m}(y-D)]}, \quad y > D, \quad (7)$$

$$u(x, y) = \sum_{m=-\infty}^{+\infty} C_{b,m} e^{i[\alpha_m x - \beta_{b,m}y]}, \quad y < 0, \quad (8)$$

where $C_{t,m}$ and $C_{b,m}$ are unknown coefficients, and

$$\alpha_m = \frac{2\pi m}{L}, \quad \beta_{t,m} = \sqrt{k_0^2 n_t^2 - \alpha_m^2}, \quad \beta_{b,m} = \sqrt{k_0^2 n_b^2 - \alpha_m^2}. \quad (9)$$

If we define the linear operators \mathbf{B}_t and \mathbf{B}_b satisfying

$$\mathbf{B}_t e^{i\alpha_m x} = i\beta_{t,m} e^{i\alpha_m x}, \quad (10)$$

$$\mathbf{B}_b e^{i\alpha_m x} = -i\beta_{b,m} e^{i\alpha_m x} \quad (11)$$

for all integer m , then the outgoing radiation boundary conditions are

$$\frac{\partial u}{\partial y} = \mathbf{B}_t u, \quad \text{on } y = D^+, \quad (12)$$

$$\frac{\partial u}{\partial y} = \mathbf{B}_b u, \quad \text{on } y = 0^-. \quad (13)$$

In summary, a 2D periodic LEP is to find k_0 , γ , and a non-zero u satisfying Eqs. (4) or (5), (12), (13), and the following periodic condition

$$u(x + L, y) = u(x, y), \quad \text{for all } x, y. \quad (14)$$

Notice that the problem has been formulated on the rectangle given by $0 < x < L$ and $0 < y < D$.

3. Dirichlet-to-Neumann map method

To solve the non-conventional eigenvalue problem (4) or (5) and (12-14), we first reformulate the problem as Eq. (1), where \mathbf{F} is an operator and \mathbf{u} is a vector for the eigenfunction u on a few line segments. When the line segments are discretized, \mathbf{u} becomes a vector and \mathbf{F} is approximated by a square matrix. The eigenvalue problem can be solved iteratively by searching the pair (k_0, γ) , such that the matrix $\mathbf{F}(k_0, \gamma)$ is singular, then \mathbf{u} is the eigenvector of $\mathbf{F}(k_0, \gamma)$ corresponding to the zero eigenvalue.

To describe the procedure that gives rise to the reformulation (1) more clearly, we consider

the special case shown in Fig. 1, that is, the structure consists of three infinite periodic cylinder arrays. One period (i.e., $0 < x < L$) of the structure is shown in Fig. 2. and it consists of

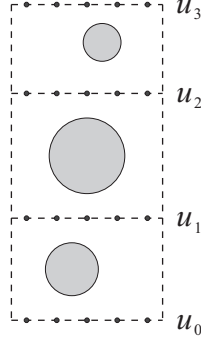


Figure 2. One period with three rectangular cells and $N = 5$ sampling points on each horizontal edge.

three rectangular cells Ω_1 , Ω_2 and Ω_3 each containing one circular cylinder. The horizontal line segments bounding or separating the rectangular cells are located at $0 = y_0 < y_1 < y_2 < y_3 = D$. Let $u_j = u(x, y_j)$ for $0 < x < L$ and $j = 0, 1, 2, 3$, then \mathbf{u} in Eq. (1) is the column vector for u_0 , u_1 , u_2 and u_3 . If each line segment (i.e., $0 < x < L$ for a fixed y_j) is discretized by N points, then \mathbf{u} and $\mathbf{F}(k_0, \gamma)$ are approximated by a column vector of length $4N$ and a $(4N) \times (4N)$ matrix, respectively.

To obtain the reformulated eigenvalue problem (1), we need the DtN maps of the rectangular cells. Consider the first cell Ω_1 given by $0 < x < L$ and $y_0 < y < y_1$, its DtN map is an operator $\mathbf{\Lambda}^{(1)}$ that maps u to its normal derivative on the boundary of Ω_1 . More precisely, $\mathbf{\Lambda}^{(1)}$ satisfies

$$\mathbf{\Lambda}^{(1)} \begin{bmatrix} u_0 \\ v_0 \\ u_1 \\ v_1 \end{bmatrix} = \begin{bmatrix} \partial_y u_0 \\ \partial_x v_0 \\ \partial_y u_1 \\ \partial_x v_1 \end{bmatrix}, \quad (15)$$

where v_0 and v_1 denote u on the two vertical edges of Ω_1 , i.e., $v_0 = u(0, y)$ and $v_1 = u(L, y)$ for $y_0 < y < y_1$, $\partial_y u_0$ denotes $\partial_y u$ on the bottom edge of Ω_1 , etc. For a cell containing a circular cylinder, the DtN map can be constructed from cylindrical wave expansions. The details are given in [15]. If we further apply the periodic conditions

$$v_1 = v_0, \quad \partial_x v_1 = \partial_x v_0, \quad (16)$$

then v_0 and v_1 can be eliminated. This leads to the reduced DtN map $\mathbf{M}^{(1)}$ satisfying

$$\mathbf{M}^{(1)} \begin{bmatrix} u_0 \\ u_1 \end{bmatrix} = \begin{bmatrix} \partial_y u_0 \\ \partial_y u_1 \end{bmatrix}. \quad (17)$$

For the other two cells Ω_2 and Ω_3 , we can similarly find the reduced DtN maps $\mathbf{M}^{(2)}$ and $\mathbf{M}^{(3)}$. These are 2×2 matrix operators. We can write them down in block form as

$$\mathbf{M}^{(j)} = \begin{bmatrix} \mathbf{M}_{11}^{(j)} & \mathbf{M}_{12}^{(j)} \\ \mathbf{M}_{21}^{(j)} & \mathbf{M}_{22}^{(j)} \end{bmatrix} \quad (18)$$

for $j = 1, 2, 3$. If each horizontal line segment is discretized by N points, then $\mathbf{M}^{(j)}$ is a $(2N) \times (2N)$ matrix and its blocks are $N \times N$ matrices.

The final linear system (1) is obtained by matching $\partial_y u$ on the horizontal line segments. For example, at $y = y_0$, we can evaluate $\partial_y u$ from the boundary condition (13) and by the reduced DtN map $\mathbf{M}^{(1)}$, that is

$$\partial_y u_0 = \mathbf{B}_b u_0 = \mathbf{M}_{11}^{(1)} u_0 + \mathbf{M}_{12}^{(1)} u_1.$$

At $y = y_1$, we can evaluate $\partial_y u$ by $\mathbf{M}^{(1)}$ and $\mathbf{M}^{(2)}$, thus

$$\partial_y u_1 = \mathbf{M}_{21}^{(1)} u_0 + \mathbf{M}_{22}^{(1)} u_1 = \mathbf{M}_{11}^{(2)} u_1 + \mathbf{M}_{12}^{(2)} u_2.$$

The matrix \mathbf{F} in (1) is obtained by assembling all these equations together. We have

$$\mathbf{F} = \begin{bmatrix} \mathbf{M}_{11}^{(1)} - \mathbf{B}_b & \mathbf{M}_{12}^{(1)} & 0 & 0 \\ -\mathbf{M}_{21}^{(1)} & \mathbf{M}_{11}^{(2)} - \mathbf{M}_{22}^{(1)} & \mathbf{M}_{12}^{(2)} & 0 \\ 0 & -\mathbf{M}_{21}^{(2)} & \mathbf{M}_{11}^{(3)} - \mathbf{M}_{22}^{(2)} & \mathbf{M}_{12}^{(3)} \\ 0 & 0 & -\mathbf{M}_{21}^{(3)} & \mathbf{B}_t - \mathbf{M}_{22}^{(3)} \end{bmatrix}. \quad (19)$$

Notice that the operators \mathbf{B}_t and \mathbf{B}_b depend on k_0 , and $\mathbf{M}^{(j)}$, $j = 1, 2, 3$, depend on k_0 and γ , therefore \mathbf{F} depend on k_0 and γ .

Clearly, if the number of cells in one period is J (instead of 3), we have $J + 1$ horizontal edges, then the matrix \mathbf{F} has $(J + 1) \times (J + 1)$ blocks. For large J , the method based on this \mathbf{F} becomes less efficient. Fortunately, there is an alternative formulation where the matrix \mathbf{F} is independent of J .

Using the reduced DtN maps $\mathbf{M}^{(1)}$ and $\mathbf{M}^{(2)}$ for Ω_1 and Ω_2 , respectively, we can eliminate u_1 to obtain the combined reduced DtN map $\mathbf{M}^{(1,2)}$ for the union of Ω_1 and Ω_2 . The operator

$\mathbf{M}^{(1,2)}$ satisfies

$$\mathbf{M}^{(1,2)} \begin{bmatrix} u_0 \\ u_2 \end{bmatrix} = \begin{bmatrix} \partial_y u_0 \\ \partial_y u_2 \end{bmatrix}. \quad (20)$$

The elimination procedure is straightforward and it is similar to the one given in [23]. The process can be easily continued. From $\mathbf{M}^{(1,2)}$ and $\mathbf{M}^{(3)}$, we can find the reduced DtN map $\mathbf{M}^{(1,2,3)}$ that links u_0 and u_3 with their y derivatives. In general, if one period has J cells, we can find the reduced DtN map $\mathbf{M}^{(1,\dots,J)}$ satisfying

$$\mathbf{M}^{(1,\dots,J)} \begin{bmatrix} u_0 \\ u_J \end{bmatrix} = \begin{bmatrix} \partial_y u_0 \\ \partial_y u_J \end{bmatrix}. \quad (21)$$

Here, we assume $y_0 = 0$ and $y_J = D$ and denote $u(x, D)$ by u_J . Matching $\partial_y u$ at $y = 0$ and $y = D$, we obtain Eq. (1), where \mathbf{u} is the column vector for u_0 and u_J , and

$$\mathbf{F} = \begin{bmatrix} \mathbf{M}_{11}^{(1,\dots,J)} - \mathbf{B}_b & \mathbf{M}_{12}^{(1,\dots,J)} \\ -\mathbf{M}_{21}^{(1,\dots,J)} & \mathbf{B}_t - \mathbf{M}_{22}^{(1,\dots,J)} \end{bmatrix}. \quad (22)$$

In the above, $\mathbf{M}_{jk}^{(1,\dots,J)}$ ($1 \leq j, k \leq 2$) is the (j, k) block of $\mathbf{M}^{(1,\dots,J)}$. Notice that if each line segment is discretized by N points, \mathbf{F} given in (22) is a $(2N) \times (2N)$ matrix for any J .

If all rectangular cells are identical, we can use the recursive-doubling procedure [24] to further speed up the process. Namely, we can combine $\mathbf{M}^{(1)} = \mathbf{M}^{(2)}$ to find $\mathbf{M}^{(1,2)}$, combine $\mathbf{M}^{(1,2)} = \mathbf{M}^{(3,4)}$ to find $\mathbf{M}^{(1,\dots,4)}$, combine $\mathbf{M}^{(1,\dots,4)} = \mathbf{M}^{(5,\dots,8)}$ to find $\mathbf{M}^{(1,\dots,8)}$, etc.

A non-zero solution \mathbf{u} for Eq. (1) can only exist when the matrix \mathbf{F} is singular. Thus, we can solve k_0 and γ from a condition that \mathbf{F} is singular. Such a condition may be $\det(\mathbf{F}) = 0$, but the determinant is not a good measure for the singularity of a matrix. The smallest eigenvalue in magnitude or the smallest singular value are better choices for numerical stability reasons [25]. We choose to use the smallest singular value σ_1 , and solve k_0 and γ from

$$\sigma_1(\mathbf{F}) = 0. \quad (23)$$

Although two real parameters (k_0 and γ) are involved, we are mainly interested in those solutions with a small γ . Clearly, this is a nonlinear method and an iterative method is needed. To find an initial guess, we first set $\gamma = 0$ and find the minimum of σ_1 along the real k_0 axis. If that minimum is reached at $k_0^{(0)}$, we then find the minimum of σ_1 on the line of positive γ with fixed $k_0 = k_0^{(0)}$. If this second minimum is reached at $\gamma^{(0)}$, then $(k_0^{(0)}, \gamma^{(0)})$ is our initial guess for solving k_0 and γ from Eq. (23).

4. Numerical examples

In this section, we present some numerical examples to valid our method and to illustrate its accuracy and efficiency. The first example is a single array of circular cylinders previously analyzed by Byelobrov *et al.* [9]. The refractive indices of the cylinders and the surrounding medium (air) are $\eta = 1.4142$ and $\eta = 1$, respectively. The cylinders are made of active material and are uniformly pumped, thus $\Gamma = 1$ in the cylinders and $\Gamma = 0$ otherwise. The period of the array and the radius of the cylinders are L and R , respectively. As in [9], we calculate the lasing eigenmodes for $2 < L/R \leq 8$. The eigenpairs (k_0, γ) satisfying $k_0 L / (2\pi) \leq 1$ are shown in Figs. 3 and 4

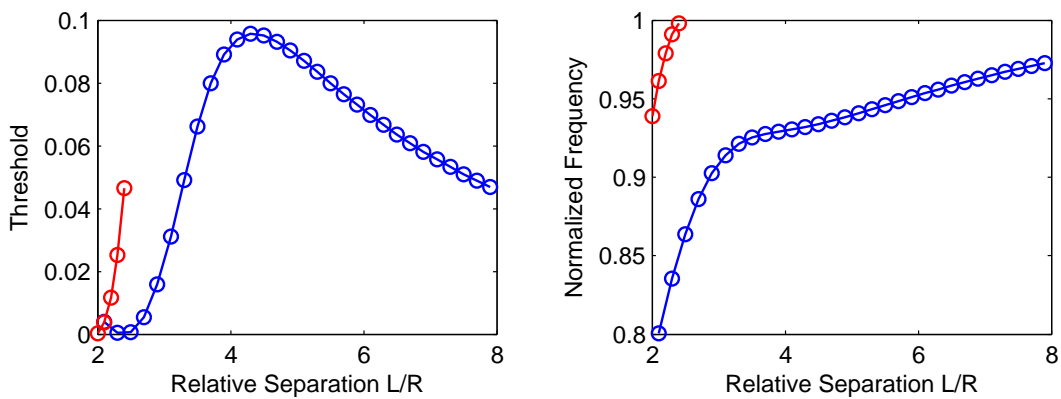


Figure 3. Gain threshold γ and normalized frequency $k_0 L / (2\pi)$ for different values of L/R and the E polarization.

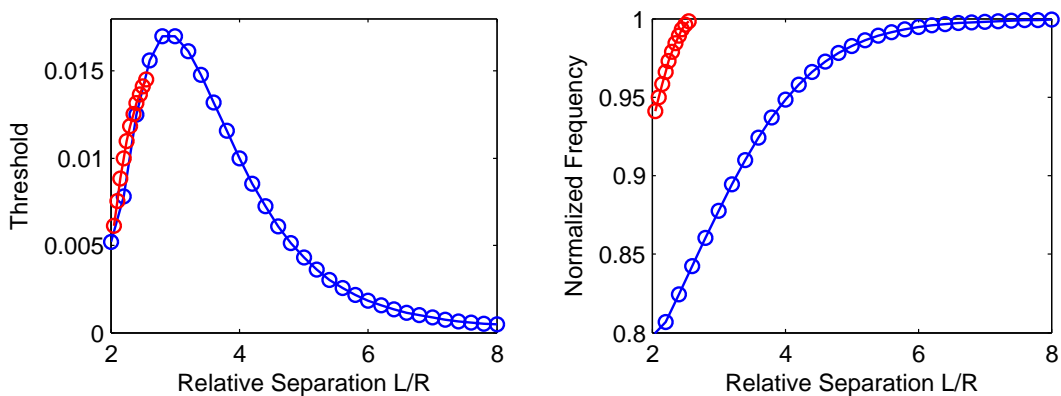


Figure 4. Gain threshold γ and normalized frequency $k_0 L / (2\pi)$ for different values of L/R and the H polarization.

for the E and H polarizations, respectively. For each polarization, we show two eigenmodes of different symmetry. The anti-symmetric mode exists for all values of L/R , while the symmetric mode only exists for smaller values of L/R . Our results shown in these two figures are obtained using $N = 6$ points on each horizontal edge, and they show good agreement with those presented in [9]. Our method is efficient, since the size of the final matrix \mathbf{F} is only 12×12 .

For this example, we test the convergence of the eigenvalue pair with respect to the number of points N for a fixed relative separation $L/R = 2.1$. A reference solution $k_0L/(2\pi) = 0.80095051$ and $\gamma = 0.003946497$ is first obtained using $N = 29$, and it is nearly identical to the solution obtained with $N = 30$. Using this reference solution, we calculate the relative errors for solutions obtained with smaller values of N . The results are plotted in Fig. 5. It is clear that for $N = 6$,

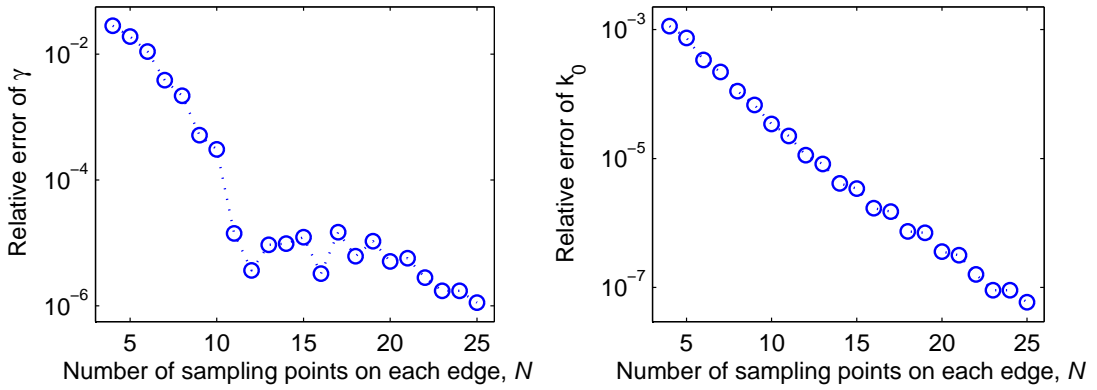


Figure 5. Convergence of γ and k_0 (or ω) with respect to N for $L/R = 2.1$.

the relative errors for γ and k_0 are less than 0.01 and 0.0005, respectively.

The second example consists of $J = 32$ identical, infinite and periodic arrays of circular cylinders surrounded by air. The radius and refractive index of the cylinders are $R = 0.3L$ and $\eta = \sqrt{2}$, respectively. The LEP for this structure was first studied by Inoue *et al.* [26]. These authors use the second model given in (3), i.e., a negative imaginary part is added to the dielectric constant (instead of the refractive index) to represent the material gain in the active region. They calculate the transmittance of the structure for a normal incident plane wave for k_0 and γ in a given region, and identify the eigenvalue pair of a lasing mode as a peak of the transmittance. This approach is not very efficient, since it is necessary to repeat the calculation for numerous points in the $k_0\gamma$ plane. We apply our method to this problem. Since J is not small, we use the alternative formulation where \mathbf{F} is given in Eq. (22). Fig. 6 shows how we obtain the initial guesses for solving (23). First, we set $\gamma = 0$ and search the local minima of $\sigma_1(\mathbf{F})$ on the real axis of k_0 (or normalized frequency $k_0L/(2\pi)$). We found three local minima as indicated by the small circles A, B and C in the first subplot of Fig. 6. The normalized frequencies for points A, B and C are $k_0L/(2\pi) = 0.39984$, 0.40736 and 0.39200 , respectively. Next, we find a minimum of $\sigma_1(\mathbf{F})$ as a function of γ for a fixed k_0 corresponding to each of the three points A, B and C. The results are indicated by the small squares in the other three subplots of Fig. 6, and their values are $(k_0L/(2\pi), \gamma) = (0.39984, 0.012)$, $(0.40736, 0.004)$ and $(0.39200, 0.023)$, respectively. With these initial guesses, we solve Eq. (23) and find three lasing

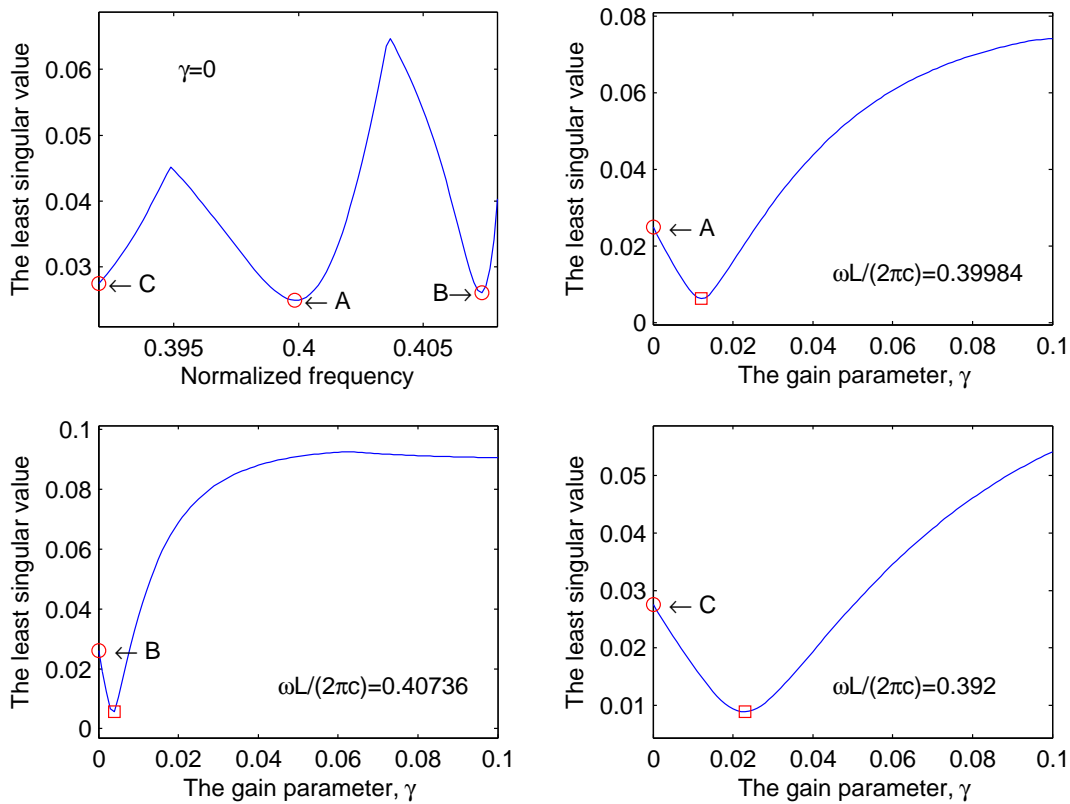


Figure 6. Local minimums give initial guesses for iterations.

eigenmodes with $(k_0L/(2\pi), \gamma) = (0.40041, 0.01214)$, $(0.40750, 0.00363)$ and $(0.39065, 0.02209)$. The mode with the normalized frequency $k_0L/(2\pi) = 0.40750$ has the lowest lasing threshold. These results are obtained with $N = 10$. Our method is efficient, since a recursive-doubling procedure is used to find $\mathbf{M}^{(1, \dots, 32)}$, and the matrix \mathbf{F} is only 20×20 .

5. Conclusion

In the previous sections, we presented an efficient method for analyzing LEPs of periodic arrays of cylinders based on the DtN-map formalism. The LEP [4, 5] is an interesting non-conventional eigenvalue problem that allows one to determine the frequency and gain threshold for lasing directly. Since gratings and photonic crystals are widely used in light-emitting devices, LEPs for periodic structures are also interesting [9, 26]. Although the governing equations are still linear, a LEP cannot be approximated by a standard linear matrix eigenvalue problem. In our method, the eigenvalues are determined from the condition that the smallest singular value of a matrix \mathbf{F} is zero. The matrix \mathbf{F} is efficiently calculated for periodic structures involving circular cylinders, and the size of \mathbf{F} is small even when the structure contains many arrays. Like the multipole

method [9], we make use of the fast converging cylindrical wave expansions, but our method does not need the tedious evaluation of lattice sums and can easily handle multiple arrays of cylinders.

If the periodic structure contains non-circular cylinders, the DtN-map approach is still applicable. Instead of cylindrical wave expansions, we can use a BIE to find the DtN maps of the cells [16]. Notice that the BIE method has been applied to LEPs involving non-circular cylinders [8], but a direct extension of the standard BIE method to periodic structures is again complicated by lattice sums. This time, the lattice sums appear in the periodic Green's function required to define the boundary integral operators. On the other hand, the BIE used to calculate the DtN maps [16] involves only the standard Green's function of the homogeneous Helmholtz equation.

Acknowledgments

This research was partially supported by the National Natural Science Foundation of China (Grant No. 11026206, Tianyuan Mathematics Fund) and the Research Grants Council of Hong Kong Special Administrative Region, China (Project No. CityU 102411).

References

- [1] O. Painter, R. K. Lee, A. Scherer, A. Yariv, J. D. O'Brien, P. D. Dapkus, and I. Kim, "Two-dimensional photonic band-gap defect mode laser," *Science* **284**(5421), 1819-1821 (1999).
- [2] K. J. Vahala, "Optical microcavities," *Nature* **424**, 839-846 (2003).
- [3] M. T. Hill, Y.-S. Oei, B. Smalbrugge, Y. Zhu, T. de Vries, P. J. van Veldhoven, F. W. M. van Otten, T. J. Eijkemans, J. P. Turkiewicz, H. de Waardt, E. Jan Geluk, S.-H. Kwon, Y.-H. Lee, R. Nötzel, and M. K. Smit, "Lasing in metallic-coated nanocavities," *Nature Photonics* **1**, 589-594 (2007).
- [4] E. I. Smotrova and A. I. Nosich, "Mathematical study of the two-dimensional lasing problem for the whispering-gallery modes in a circular dielectric microcavity," *Opt. Quant. Electron.* **36**(1-3), 213-221 (2004).
- [5] E. I. Smotrova, V. O. Byelobrov, T. M. Benson, P. Sewell, J. Ctyroky, and A. I. Nosich, "Optical theorem helps understand thresholds of lasing in microcavities with active regions," *IEEE J. Quantum Electronics* **47**(1), 20-30 (2011).
- [6] A. Yariv, *Quantum Electronics*, 3rd edition, John Wiley & Sons, New York, 1987.
- [7] E. I. Smotrova, A. I. Nosich, T. M. Benson, and P. Sewell, "Threshold reduction in a cyclic photonic molecule laser composed of identical microdisks with whispering-gallery modes," *Opt. Lett.* **31**(7), 921-923 (2006).
- [8] E. I. Smotrova, J. Ctyroky, T. M. Benson, P. Sewell, and A. I. Nosich, "Optical fields of the lowest modes in a uniformly active thin sub-wavelength spiral microcavity," *Opt. Lett.* **34**(24), 3773-3775 (2009).
- [9] V. O. Byelobrov, J. Ctyroky, T. M. Benson, R. Sauleau, A. Altintas, and A.I. Nosich, "Low-threshold lasing eigenmodes of an infinite periodic chain of quantum wires," *Opt. Lett.* **35**(21), 3634-3636 (2010).
- [10] H. Yasumoto, *Electromagnetic Theory and Applications for Photonic Crystals*, Taylor & Francis Group, New York, 2006.
- [11] C. M. Linton, "Lattice sums for the Helmholtz equation," *SIAM Review* **52**(2), 630-674 (2010).

- [12] S. Li and Y. Y. Lu, "Accurate multipole analysis for leaky microcavities in two-dimensional photonic crystals," *IEEE Photonics Technology Letters* **22**(2), 94-96 (2010).
- [13] J. Wiersig, "Boundary element method for resonances in dielectric microcavities," *J. Opt. A: Pure Appl. Opt.* **5**, 53-60 (2003).
- [14] S. V. Boriskina, P. Sewell, T. M. Benson, and A. I. Nosich, "Accurate simulation of two-dimensional optical microcavities with uniquely solvable boundary integral equations and trigonometric Galerkin discretization," *J. Opt. Soc. Am. A* **21**, 393-402 (2004).
- [15] Y. Huang and Y. Y. Lu, "Scattering from periodic arrays of cylinders by Dirichlet-to-Neumann maps," *J. Lightw. Technol.* **24**, 3448-3453 (2006).
- [16] J. Yuan, Y. Y. Lu and X. Antoine, "Modeling photonic crystals by boundary integral equations and Dirichlet-to-Neumann maps," *J. Comput. Phys.* **227**(9), 4617-3629 (2008).
- [17] Z. Hu and Y. Y. Lu, "Improved Dirichlet-to-Neumann map method for modeling extended photonic crystal devices," *Opt. Quant. Electron.* **40**, 921-932 (2008).
- [18] Y. Wu and Y. Y. Lu, "Dirichlet-to-Neumann map method for analyzing crossed arrays of circular cylinders," *J. Opt. Soc. Am. B* **26**(11), 1984-1993 (2009).
- [19] Z. Hu and Y. Y. Lu, "A simple boundary condition for terminating photonic crystal waveguides," *J. Opt. Soc. Am. B* **29**(6), 1356-1360 (2012).
- [20] L. Yuan and Y. Y. Lu, "Efficient numerical method for analyzing optical bistability in photonic crystal microcavities," *Opt. Express* **21**(10), 11952-11964 (2013).
- [21] S. Li and Y. Y. Lu, "Efficient method for analyzing leaky cavities in two-dimensional photonic crystals," *J. Opt. Soc. Am. B* **26**(12), 2427-2433 (2009).
- [22] G. Bao, D. C. Dobson and J. A. Cox, "Mathematical studies in rigorous grating theory," *J. Opt. Soc. Am. A* **12**, 1029-1042 (1995).
- [23] Y. Huang and Y. Y. Lu, "Modeling photonic crystals with complex unit cells by Dirichlet-to-Neumann maps," *Journal of Computational Mathematics* **25**(3), 337-349 (2007).
- [24] L. Yuan and Y. Y. Lu, "A recursive doubling Dirichlet-to-Neumann map method for periodic waveguides," *J. Lightw. Technol.* **25**, 3649-3656 (2007).
- [25] G. H. Golub and C. F. Van Loan, *Matrix Computation*, 3rd edition, The Johns Hopkins University Press, 1996.
- [26] K. Inoue, K. Ohtaka, and S. Noda, "Interaction between light and matter in photonic crystals," *Photonic Crystals: Physics, Fabrication, and Applications*, Springer, 222-226 (2004).